Potassium regulates the growth and toxin biosynthesis of *Microcystis aeruginosa*☆

Yixin He [a,1], Jianrong Ma [b,1], Vanderwall Joseph [c], Yanyan Wei [d], Mengzi Liu [a], Zhaoxue Zhang [a], Guo Li [a], Qiang He [a], Hong Li [a,*]

[a] *Key Laboratory of Eco-Environment of Three Gorges Region, Ministry of Education, Chongqing University, Chongqing, 400044, China*
[b] *CAS Key Laboratory of Reservoir Environment, Chongqing Institute of Green and Intelligent Technology, Chinese Academy of Sciences, Chongqing, 400714, China*
[c] *Flathead Lake Biological Station, University of Montana, Polson, MT, 59860, USA*
[d] *Cultivation Base of Guangxi Key Laboratory for Agro-Environment and Agro-Products Safety, College of Agriculture, Guangxi University, Nanning, 530004, China*

ARTICLE INFO

ABSTRACT

Potassium (K^+) is the most abundant cation in phytoplankton cells, but its impact on *Microcystis aeruginosa* (*M. aeruginosa*) has not been fully documented. This study presents evidence of how K^+ availability affects the growth, oxidative stress and microcystin (MC) production of *M. aeruginosa*. The iTRAQ-based proteomic analysis revealed that during K^+ deficiency, serious oxidative damage occurred and the photosynthesis-associated and ABC transporter-related proteins in *M. aeruginosa* were substantially downregulated. In the absence of K^+, a 69.26% reduction in cell density was shown, and both the photosynthesis and iron uptake were depressed, which triggered a declined production of ATP and expression of MC synthetases genes (*mcy*A, B and D), and MC exporters (*mcy*H). Through the impairment of both the MC biosynthesis and MC transportation out of cells, K^+ depletion caused an 85.89% reduction of extracellular MC content at the end of the study. However, with increasing in the available K^+ concentrations, photosynthesis efficiency, the expression of ABC-transporter proteins, and the transcription of *mcy* genes displayed slight differences compared with those in the control group. This work represents evidence that K^+ availability can regulate the physiological metabolic activity of *M. aeruginosa* and K^+ deficiency leads to depressed growth and MC production in *M. aeruginosa*.

© 2020 Elsevier Ltd. All rights reserved.

1. Introduction

Harmful algal blooms (HABs) represent a worldwide environmental issue in freshwater ecosystems across the world and are generally caused by cyanobacteria (Sheng et al., 2019; Yan et al., 2017). HABs are harmful because of toxics production (Smith and Daniels, 2018). Microcystin (MC), the most commonly detected cyanotoxin produced by *Microcystis*, can promote tumor production in both liver and pancreatic tissues (Du et al., 2019; He et al., 2018). MC is synthesized non-ribosomally by 10 proteins (mcyA-J) encoded by the *mcy* gene cluster, in which *mcy*A encodes MC synthetase,

and *mcy*D is involved in the synthesis of the β-amino acid Adda that underlies the toxicity of all variants of MC, and *mcy*H is linked to the MC biosynthesis pathway and is considered as an transporter for MC release (Zhou et al., 2017). The synthesis of MC requires energy and is regulated by a variety of factors such as light intensity and available iron concentration (Fontanillo and Köhn, 2018).

The increasing frequency of HABs worldwide is pushing authorities to find solutions for new mitigation avenues, including those related to cell growth management (Barros et al., 2019). Cyanobacteria growth can be severely affected by the environmental parameters such as temperature (Knutson et al., 2018), dissolved oxygen levels (Chen et al., 2016), pH (Beklioglu and Moss, 2010) and key nutrient availability (Fu et al., 2019). For decades, the limnologists made great endeavor in studying the role on nutrients, mainly focused on nitrogen, phosphorus and iron on the growth of cyanobacteria (Bai et al., 2017; Seip, 1994; Wang et al., 2014). However, the impact of potassium (K^+), a physiologically unique

metabolic cofactor and osmolyte (Jaworski et al., 2003), on phytoplankton growth has scarcely been investigated (Talling, 2010). Nevertheless, previous studies have demonstrated that the variations in the available K^+ concentration can cause severe physiological changes in phytoplanktonic cells. For example, K^+ concentrations below 383.65 μM and 76.73 μM substantially inhibits the growth of *Chlorella pyrenoidosa* and *Synurophytes*, respectively (Plato and Denovan, 1974; Sandgreen, 1988). In contrast with the above results, no significant differences in the growth rate and final biomass of the diatoms *Asterionella formosa* and *Diatoma elongatum* were observed at K^+ concentrations of 0.7−3.2 μM (Jaworski et al., 2003). The response of phytoplankton to K^+ exposure seems to be dose- and species-dependent, which could be due to both the K^+ requirement of phytoplankton and the K^+ concentration in the environment (Winter et al., 1987). With respect to *Microcystis*, a previous study demonstrated that a K^+ concentration of 6 mM induced a 50% reduction in *Microcystis* biomass, likely because K^+ was involved in the rapid extrusion of sodium from *Microcystis* cells which subsequently led to a disturbance in osmosis (Shukla and Rai, 2006). The above-mentioned literatures clearly indicated that potassium availability may impact the growth of phytoplankton in terms of growth rate, while the physiological and metabolic responses within the phytoplanktonic cells is lacking.

In this study, toxin-producing *Microcystis aeruginosa* (*M. aeruginosa*), which is the most widespread HABs species recorded in freshwater, was used to assess the role of K^+ in growth regulation, oxidative response, morphological and physiological alternation, with special attention to MC biosynthesis, during which quantitative Real-time PCR (qRT-PCR) and isobaric tagging for relative and absolute quantification (iTRAQ)-based quantitative proteomics methods were used. The objectives of this study are to identify the influence of available K^+ concentrations on *M. aeruginosa* growth, evaluate the impact of different K^+ concentrations on the toxin-producing capability of *M. aeruginosa,* and identify the potential mechanism underlying these changes.

2. Materials and methods

2.1. Cultivation of M. aeruginosa

M. aeruginosa (FACHB-905) was provided by the Freshwater Algae Culture Collection at the Institute of Hydrobiology (FACHB-Collection, Wuhan, China). To thrive, cultured *M. aeruginosa* requires concentrations of K^+ above critical concentrations in culture media (Brdjanovic et al., 1996). In BG-11 medium, which is commonly used for the isolation and culture of freshwater microalgae, the K^+ concentration is set at 0.46 mM (Qiu et al., 2013). In this study, *M. aeruginosa* was cultured in BG-11 medium in a growth chamber for 30 days until reaching the stable growth stage. To evaluate the dose-dependent response to varied K^+ concentration, 5 mL of the cultured *M. aeruginosa* was incubated in flasks of BG-11 medium containing K^+ concentrations of 0, 0.23 mM, 0.46 mM, and 0.92 mM, with triplicates for each concentration. During the preparation of the mediums, K_2HPO_4 was used as both a K^+ and phosphorus source to generate final K^+ and phosphorus concentrations of 0.46 mM (used as the control) in BG-11 medium. With respect to the absence of K^+ ($K^+ = 0$ mM), Na_2HPO_4 instead of K_2HPO_4 was used to generate a favorable concentration of phosphorus that equal to that in the BG-11 medium. To incubate the *M. aeruginosa* in medium with $K^+ = 0.23$ mM, half of the amount of K_2HPO_4 relative to that in BG-11 medium was added, and the excessive phosphorus was provided by Na_2HPO_4. For the medium in which $K^+ = 0.92$ mM, an amount of K_2HPO_4 equal to that in BG-11 medium was used, and then the excessive K^+ was added with

KCl. The initial density of *M. aeruginosa* of all the treatments was maintained at approximately 3.29×10^5 cells/ml. Incubation tests were performed in triplicate under controlled laboratory conditions (25 ± 1 °C, 40 mmol photons/(m^2/sec) and a 12 h/12 h (light/dark) cycle). During the study, the flasks were shaken manually every day.

The cell density of *M. aeruginosa* was assessed every 3 days. Briefly, 0.1 mL of each phytoplankton samples was placed in a 20 mm × 20 mm settling chambers and enumerated by light microscopy at 400 magnification (Zeiss Axiovert 200M). Specific growth rate (μ) was calculated by using the following equations:

$$\mu = (in\ X_2 - inX_1) / (t_2 - t_2)$$

X_2 and X_1 represent the cell density at times t_2 and t_1, respectively.

To evaluate the dynamic change of the *M. aeruginosa* growth, pulse-amplitude-modulated fluorometer AquaPen-C AP-C 100 (Photon Systems Instruments, Czech Republic) equipped with a FluorPen 1.0 software was employed to measure the maximal photochemical efficiency of PSII (Fv/Fm) of *M. aeruginosa* every 6 days during the experiment.

2.2. Detection of superoxide dismutase (SOD) activity and malonaldehyde (MDA) content

The intracellular SOD activity and MDA content and total protein content were examined every 6 days using SOD assay kit, MDA assay kit and total protein content assay kit according to the manufacturer's protocol of Nanjing Jiancheng Bioengineering Institute (Nanjing, China), respectively. Briefly, 20 mL algal cell cultures were centrifuged at 8000 rpm for 15 min at 4 °C. Cell pellets were resuspended in 2 mL PBS (pH7.8) and then disrupted by freeze-thawing with liquid nitrogen. The homogenates were used for total protein content assay and were then centrifuged at 12,000 rpm for 15 min at 4 °C. The supernatants were collected for enzyme activity assays. The SOD activity, MDA content and total protein content in algal cells were determined using a Multiskan spectrum (ELX808, BioTek, USA) at wavelengths of 450 nm, 532 nm and 562 nm, respectively. Finally, the SOD activity and MDA content were normalized with total protein content. Moreover, the content of intracellular Ferredoxin (Fd) and triphosadenine (ATP) synthase, which were closely related to the energy supply of the MC-producing process (Buckel and Thauer, 2013), were synchronously measured with the supernatants from the homogenates using Ferredoxin ELISA Kit and ATP synthase ELISA Kit (Camilo biological ELISA Kit) according to the manufacturer's protocol of Nanjing Camilo biological engineering co.LTD (Nanjing, China).

2.3. Measurement of extracellular and intracellular MC concentrations

MC within *M. aeruginosa* cells is called intracellular MC (IMC). MC within *M. aeruginosa* cells will be released into surrounding waters and become extracellular MC (EMC) when cells grow or lyse. Following the same interval of enzyme activities measurement, 20 mL of algal solution were firstly centrifuged at 8000 g at 4 °C for 10 min and the supernatant was filtered through a 0.22 mm glass fiber membrane. The filtrate was used for the assay of the EMC. The cell pellets were re-suspended in 1 mL ddH$_2$O, frozen-thawed three times, and then centrifuged at 4000 g for 15 min, and the supernatant was used for the determination of the concentration of IMC. The concentrations of MC in the samples were measured by the Microcystin ELISA Kit produced by Jiangsu Meimian industrial Co., Ltd (Jiangsu, Chian).

2.4. Morphological response and qRT-PCR assay

After 30 days of incubation, *M. aeruginosa* cells were collected by centrifugation at 8000 rpm (10 min) for morphological observation, toxin-gene quantification, and iTRAQ assessments. The supernatants were used for three-dimensional excitation emission matrix fluorescence spectroscopy (EEM) analysis to explore the extracellular secretion of *Microcystis aeruginosa*. The cell morphological properties were determined using transmission electron microscopy (TEM, FEI, Tecnai G2 Spirit, USA) and scanning electron microscopy (SEM, HITACHI, S4800, Japan), as previously described (Mao et al., 2018). The transcriptional abundance of four *mcy* genes (*mcy*A, *mcy*B, *mcy*D and *mcy*H) were assessed using quantitative Real-time PCR (qRT-PCR). Primer sets used for the amplification of *mcy* genes are summarized in Table S1. The relative gene expression data from qRT-PCR were evaluated by the $2^{-\triangle\triangle Ct}$ method (Livak and Schmittgen, 2001). More details concerning the qRT-PCR assays are provided in the Supporting Information (SI).

2.5. iTRAQ analysis

2.5.1. Protein digestion and iTRAQ labeling

iTRAQ is a multiplexed protein quantitative strategy that provides relative and absolute measurements of proteins in complex mixtures. The approach is capable of simultaneously identifying and quantifying proteins from multiple samples (Yang et al., 2013). Description of *M. aeruginosa* protein extraction was supplied in SI. Then the protein digestion was performed and the resulting peptide mixture was labeled using the 8-plex iTRAQ reagent, following the manufacturer's instructions (Applied Biosystems, Foster City, CA, USA). More details of the iTRAQ labeling are provided in the SI.

2.5.2. Mass spectrometry analysis

Experiments were performed on a Q Exactive mass spectrometer coupled with an Easy-nLC 1200MS. A volume of 4 μl of each sample was injected for nanoLC-MS/MS analysis. More details of the nanoLC-MS/MS analysis are provided in the Supporting Information.

2.5.3. Sequence database searching

MS/MS spectra were searched using ProteinDiscover TM Software 2.1 against the transcript database of *M. aeruginosa* (http://www.uniprot.org/uniprot/?query=microcystis%20aeruginosa&sort=score). The highest score for a given peptide mass (best match to that predicted in the database) was used to identify parent proteins. The following parameters for protein searching were set: tryptic digestion with up to two missed cleavages, the carbamidomethylation of cysteines as a fixed modification, and the oxidation of methionines and protein N-terminal acetylation as variable modifications. Peptide spectral matches were validated based on q-values at a 1% false discovery rate. To display the overall trends of the specific functional categories regulated in the experimental groups, gene ontology (GO) category enrichment analysis was conducted using all differentially expressed proteins with significant differences categorized according to GO Slim classification for *M. aeruginosa* NIES-843.

2.6. Data analysis

Statistical analysis was performed using SPSS 18.0 software (SPSS Inc., Chicago, IL, USA), and data are presented as the mean ± standard deviation. Significant differences were determined using ANOVA one-way analysis of variance followed by Dunnett post hoc test for comparing the data of treatment groups against the control, and $p < 0.05$ was considered significant.

## 3. Results

3.1. M. aeruginosa growth and photosynthesis

In the absence of K^+, although the density of *M. aeruginosa* increased from 3.29×10^5 to 3.32×10^6 cells/ml, the dynamics of *Microcystis* density exhibited slight variations from day 18 (Fig. 1a). With increasing available K^+ concentrations, dual responses were observed. The K^+ concentration of 0.23 mM favored *M. aeruginosa* growth more, and the cell density was 2.31 times higher than that observed in the absence of K^+. The K^+ concentration of 0.46 mM (control) was the optimal concentration for *M. aeruginosa* growth among the tested treatments, as *M. aeruginosa* density showed a linear increase during the 30 days of incubation and reached the final density of 1.08×10^7 cells/ml, which was 3.23- and 1.39-fold higher than the densities achieved under K^+ concentrations of 0 and 0.23 mM, respectively. However, a higher K^+ concentration (0.92 mM) tended to inhibit the growth of *M. aeruginosa*, as the final cell density in the control samples was 1.25-fold higher than it. Moreover, in comparison to the normal K^+ concentration present in the BG-11 medium, the specific growth rates observed with the other three K^+ concentration treatments were relatively slower at day 3. In the K^+ absence treatment, a negative specific growth rates was recorded since day 27 (Fig. 1b). The Fv/Fm values found in this study indicate the ability of *M. aeruginosa* cells to perform photochemistry reactions with significant reduction during consecutive days of being cultured in the K^+ absence treatment (Fig. 1c). In the control group, the maximum Fv/Fm value (0.71) was noted at day 18, while the minimum Fv/Fm value (0.31) was noted in the K^+ absence treatment at the same day.

3.2. Oxidative stress

In comparison to the control group, the SOD activity of *M. aeruginosa* in the K^+ absence treatment showed a significant increase during the consecutive incubation and the highest SOD activity was noted at day 18 (Fig. 2a), which was 2.58 times of that of the control, relative less significant increase of SOD activities were shown in the K^+ = 0.23 mM and 0.92 mM treatments, and it should be noted that SOD activities at day 24 were not significantly different from the control but increased again at day 30 in the K^+ = 0.23 mM and 0.92 mM treatments. To further investigate the degree of membrane damage caused by oxidative stress, the MDA content was evaluated. As shown in Fig. 2b, significant increase in MDA level of *M. aeruginosa* was observed with varied available K^+ concentration, among which K^+ absence treatment caused the most serious MDA accumulation and the highest MDA content was noted at day 30, which was 3.87 times of the control.

3.3. Biosynthesis of MC, MC-producing related proteins, and MC-related gene transcriptions response

EMC concentrations (Fig. 3 a) tended to increase with time, but in the K^+ absence treatment, EMC concentration tended to be stable since day 18 and was detected at 0.78 μg/l at day 30, the greatest amount of EMC was released in the control group (5.53 μg/l). During the experimental period, the IMC concentrations (Fig. 3 b) in all groups started to behave differently since Day 6. It is noted that the IMC concentration remained relatively constant in K^+ absence treatment while it increased significantly ($p < 0.05$) in other 3 groups. The IMC in all treatments reached asynchronous peaks of 46.14, 72.02, 65.86 and 58.73 μg/10^9 cells in 0 mM, 0.23 mM, 0.46 mM and 0.92 mM groups, respectively. The relative Fd and ATP synthetase level were shown in Fig. 3 c-d, the Fd level at day 30 was in accordance with the iTRAQ analysis, and the highest
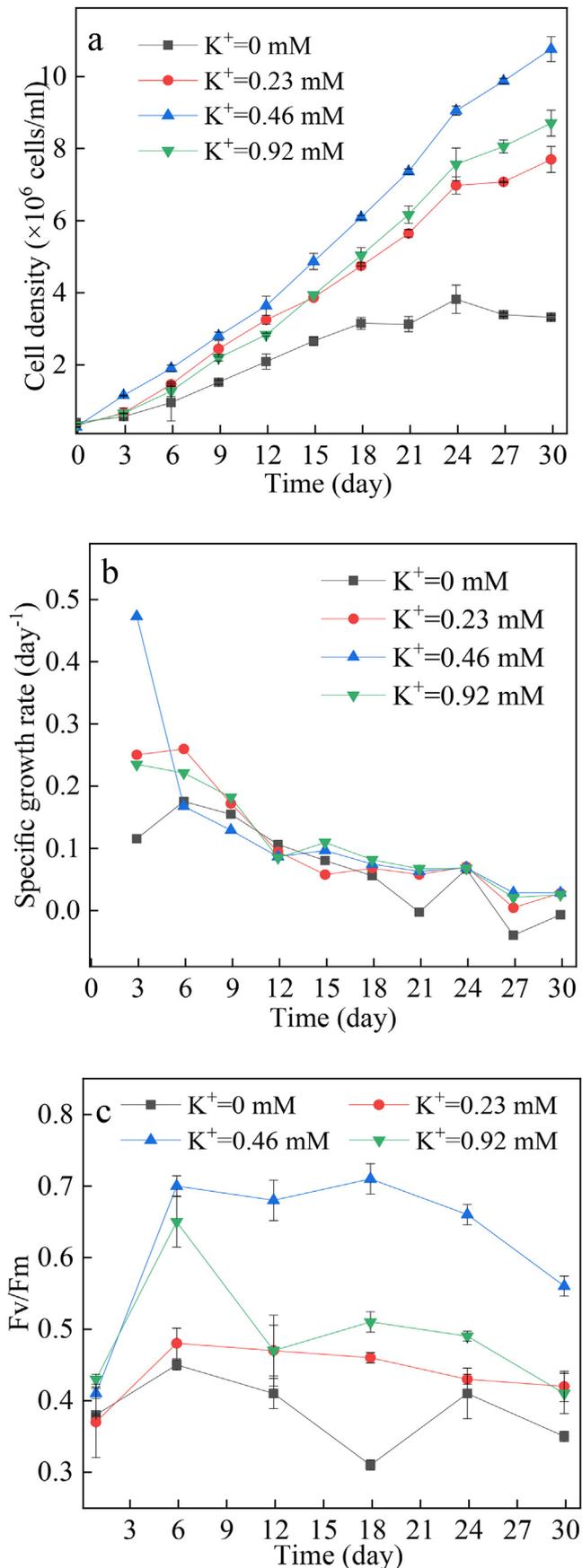
Fig. 1. Dynamics of *M. aeruginosa* growth (a, b) and Fv/FM (C) under the studied K$^+$ concentration gradients.

Fd level was noted at day 12 in the 0.92 mM treatments, which was 14% higher than then control. With respect to the ATP synthetase level, the highest ATP synthetase level was noted at day 12 in the 0.23 mM treatments, and the final ATP synthetase level in the K$^+$ absence treatment reached 50% of that in control.

At the genetic level, the relative transcriptional abundance of MC-producing genes showed a similar pattern to those of the MC concentrations. Without the addition of K$^+$, the relative transcriptional abundance reached approximately 0.37, 0.72, 0.75 and 0.54 for *mcy*A, B, D and H, respectively. The gene expressions in the K$^+$-added groups was significantly enhanced (P < 0.05, Fig. 3 e), which was consistent with the MC concentration pattern. It should be noted that when the K$^+$ concentrations were increased to 0.92 mM, *mcy* gene expression was augmented.

3.4. Proteomic responses to K$^+$ exposure

3.4.1. Protein identification and quantification in M. aeruginosa
iTRAQ-based quantitative proteome characterization of *M. aeruginosa* cells under different K$^+$ exposure levels was conducted to reveal the proteomic response of the cyanobacteria. Here, 25009 unique peptides that corresponded to 3263 proteins were identified. In comparison to the *M. aeruginosa* cells incubated in BG-11 medium, 530 proteins were upregulated and 266 proteins were downregulated in the absence of K$^+$, 61 proteins were up-regulated and 88 proteins were down-regulated with 0.23 mM K$^+$, and 144 and 127 proteins were up- and downregulated, respectively, in cells cultured in the medium containing 0.92 mM (Fig. 4). Between samples, the proteins with fold-change ratios ≥1.20 or ≤0.83 and a *p* < 0.05 were considered differentially expressed proteins (DEPs, *t*-test).

3.4.2. GO annotation of the affected proteins s and those associated with signaling KEGG pathways
iTRAQ analysis of the *M. aeruginosa* proteome revealed that among the 3263 identified proteins, 2768 proteins were annotated in the GO database, which could be categorized into diverse functional classes related to biological processes, cellular components and molecular functions (Fig. S1). KEGG analysis results showed that proteins associated with ABC transporter and photosynthesis were evidently regulated (Fig. S2). Meanwhile, numerous DEPs were mapped to ABC transporter pathways in KEGG, and it should be noted that the ABC transporter pathways in both the K$^+$ = 0 vs. K$^+$ = 0.46 mM (Fig. S3 a) and K$^+$ = 0.92 mM vs K$^+$ = 0.46 mM (Fig. S3 b) incubated *M. aeruginosa* cells were down-regulated; meanwhile, the DEPs in these experimental groups were similar. For instance, bicarbonate transport system substrate-binding protein (CmpA), iron (III) transport system substrate-binding protein (AfuA), and the associated osmoprotectant transport system substrate-binding protein (OpuBC) were all down-regulated. Table S2 shows the specific regulating-folds of the ABC transporter-related DEPs, which revealed that AfuA was down-regulated by approximately 34% and 31% in K$^+$ = 0 vs K$^+$ = 0.46 mM and in K$^+$ = 0.92 mM vs K$^+$ = 0.46 mM, respectively.

Moreover, the DEPs related to photosynthesis showed significant differences both qualitatively and quantitatively. In the absence of K$^+$, the expression patterns of most DEPs related to photosynthesis were much more complicated than those in the K$^+$ = 0.92 mM groups. Table S3 lists the photosynthesis-related DEPs in the absence of K$^+$ vs K$^+$ = 0.46 mM and in K$^+$ = 0.92 mM vs K$^+$ = 0.46 mM (19 and 2 DEPs, respectively). The DEPs in each photosynthesis subsystem in the K$^+$ absence groups are shown in Fig. S3 c, among which ferredoxin (which functions as an electron carrier between the membrane-bound iron-sulfur centers in photosystem I (PSI) (Inda and Luisa Peleato, 2003), was
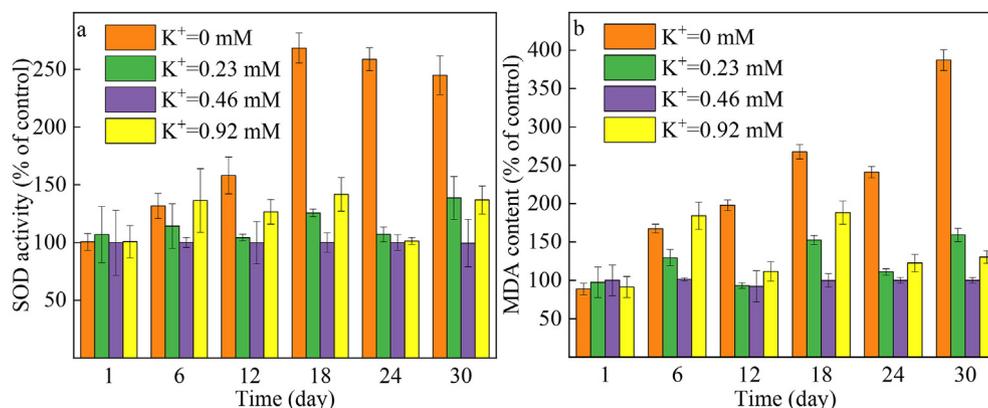
Fig. 2. Intracellular SOD activity (a) and MDA content (b) in *M. aeruginosa* cells.

down-regulated by 48%. Meanwhile, 4 proteins related to photosystem II (PSII) (photosystem II D2 protein, photosystem II protein D1, photosystem II 12 kDa extrinsic protein and photosystem II lipoprotein Psb27) were downregulated by nearly 25% (Table S3).

4. Discussion

4.1. K^+ regulates M. aeruginosa growth and cell integrity

Potassium stimulates enzyme reactions associated with the synthesis of cell materials (Brdjanovic et al., 1996). A previous study suggested that K^+ is not an essential element limiting the growth rates and biomass yields of the diatom *Asterionella formosa* (Jaworski et al., 2003). The opposite was found in this study, which confirmed that in the K^+-free medium, though the proliferation of *M. aeruginosa* was indeed observed, the growth rates were substantially depressed in comparison to those observed with incubation in BG-11 medium (Fig. 1a). A possible reason for the contradictory results between the previous study and our findings may be attributed to the different K^+ requirements of *Asterionella formosa* and *M. aeruginosa*. Additionally, the abovementioned study was performed with K^+ concentrations in the range of 0.3–6 μmol/l, which probably met the critical requirement of K^+ for the studied diatom. The role of K^+ in supporting *M. aeruginosa* can also be evidenced by the algal density dynamics and growth rate achieved in $K^+ = 0.46$ mM medium, which had the maximum values among the studied K^+ gradients. However, upon further increasing the K^+ level, the *M. aeruginosa* density was reduced by nearly 20%. Our results are in agreement with those of a previous study, which confirmed that higher K^+ concentrations depressed the growth and reduced the biomass of the chrysophyte *Dinobryon* (Talling, 2010). Nevertheless, our study showed the dual role of the available K^+ concentration in regulating the growth of *M. aeruginosa* for the first time.

The impact of the available K^+ concentration on *M. aeruginosa* can also be indicated by the morphological response of the *M. aeruginosa* cells, which clearly revealed that in comparison to *M. aeruginosa* in the control culture, the damage to cell integrity was largely enhanced without K^+ supplementation but was impaired to some extent under higher K^+ concentrations (Fig. S4). Moreover, the *M. aeruginosa* cell disruption levels produced under varied K^+ concentrations (Fig. S5), as determined by flow cytometry, showed that the population of damaged cells increased with reduced K^+ concentrations, but the negative effects seemed to be impaired by higher ambient K^+ exposure, and this observation was fully consistent with the growth dynamics and morphological response. Moreover, the results of EEM analysis, which provided

insight into the variation of *M. aeruginosa* cell constitution after discharge plasma oxidation (Zhang et al., 2014), revealed an obvious increase in fluorescence intensity from tryptophan-like substances (Ex/Em 275/320−335 nm) with the depletion of K^+ (Fig. S6). The release of extracellular proteins substantially indicated lysis of *M. aeruginosa* cells, which may be helpful for the formation of colonial *M. aeruginosa*.

4.2. K^+ effects on antioxidant condition in M. aeruginosa

Generally, SOD plays a vital role in cellular antioxidant defense, which is able to convert superoxide radicals into molecular oxygen or hydrogen peroxide (Hassan and Scandalios, 1990). In our study, in comparison to the control, the increase of SOD activity in all groups at the early stage of the experiment implied that the oxidative stress has occurred, indicating the superoxide radicals have accumulated in cells under K^+ variation. A precious study also demonstrated that K^+ starvation could induce oxidative stress in *solanum lycopersicum* (Hernandez et al., 2012). Aside from SOD, MDA also involves in the redox state in cells as it is a by-product of lipid peroxidation (Vanhoudt et al., 2011), In our study, higher MDA level co-occurred with damaged cellular surface morphology and increased cell disruption levels under K^+-limited and exceed condition, suggesting the membrane lipid peroxidation and change of membrane fluidity and permeability (Melegari et al., 2013).

4.3. K^+ deficiency impacts ABC transporters and photosynthesis

ABC transporters are members of a protein superfamily, which includes trans-membrane proteins that use the energy of adenosine triphosphate (ATP) binding and hydrolysis to carry out certain biological processes (Hu et al., 2017). Previous studies showed that ABC transporters can translocate monomers across diffusion barriers and regulate plant development by transporting plant hormones (Do et al., 2018); hence, they are imperative for the normal functioning of cell physiology. In this study, iTRAQ analysis demonstrated changes of the DEPs involved in ABC transporters (Fig. S3 a, b and Table S2). In comparison to control, the AfuA, an iron (III) transport system substrate-binding protein, was downregulated by 33% and 30% in the $K^+ = 0$ and $K^+ = 0.92$ mM treatments, respectively. Iron is necessary for the transformation of coproporphyrin into protoporphyrin (Demirel et al., 2009) and is required for various cellular processes, including photosynthesis and electron and oxygen transfer (Kobayashi et al., 2019). Therefore, with the downregulation of iron transportation, the physiological function of the cells would be seriously affected. It has been found that ABC transporters are also involved in the export of MC
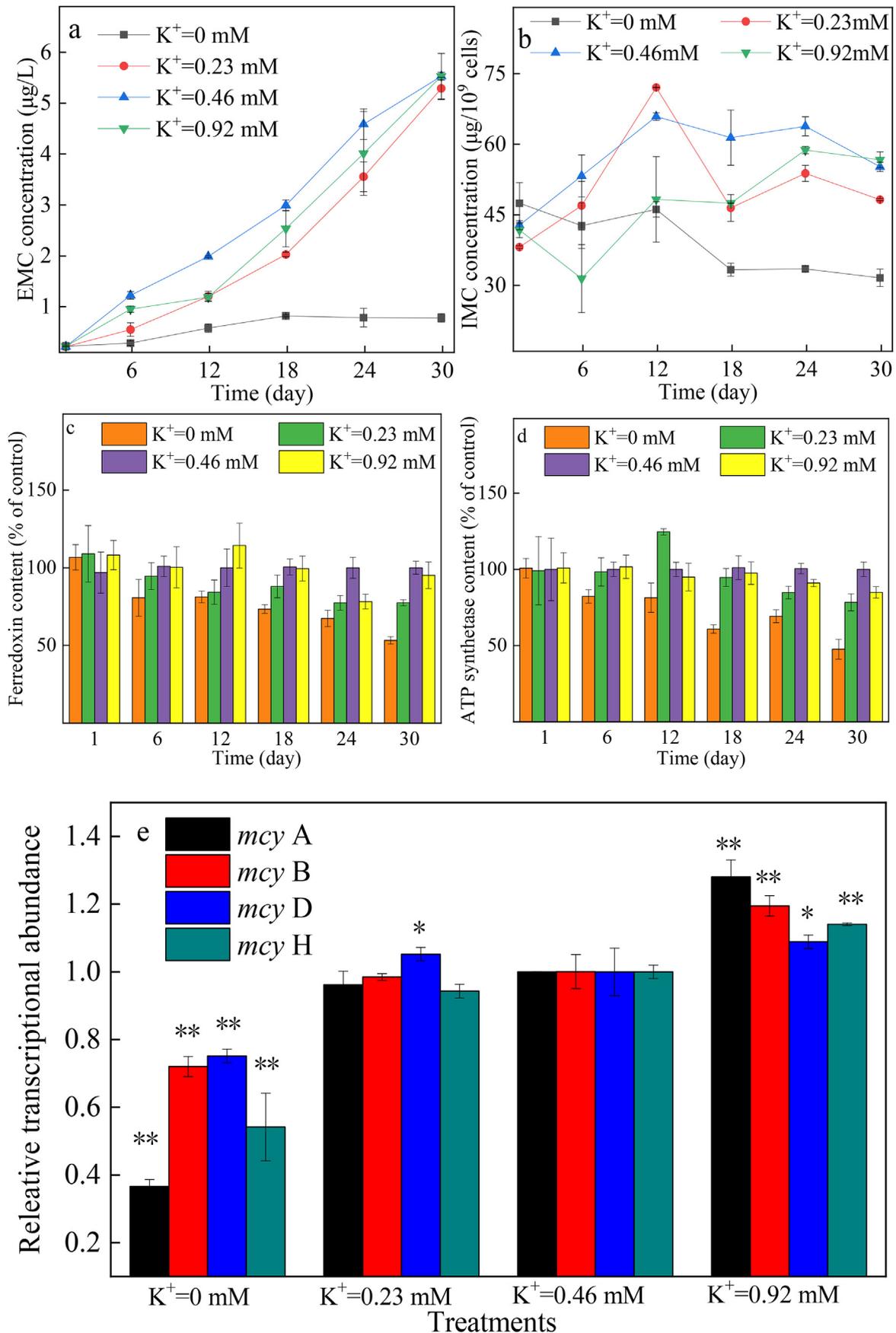
Fig. 3. Concentration of extracellular MC (a), intracellular MC (b), ferredoxin content (c), ATP synthetaseontent (d) and the relative transcriptional abundance of MC-producing genes (e) of *M. aeruginosa* exposed to varied K$^+$ concentrations.

(Pearson et al., 2004). This study observed the downregulation of several ABC transporters in K^+-absent treatments relative to the control group; hence, this effect might contribute to the decreased release of EMC (Fig. 2 a).

Photosynthesis plays a vital role as the energy source for cyanobacteria metabolism, and its efficiency can be significantly affected by the surrounding environment. The photoreaction system incorporates photosystem II (PS II), photosystem I (PS I), the light harvesting system, cytochrome b6f and ATP synthase (Zheng et al., 2018). SEM results showed that in the K^+ = 0.46 mM groups, the THY structure, wherein the primary reactions of photosynthesis in algae cells occur (Rochaix, 2007), was severely damaged (Fig. S4). Hence, the destroyed THY structure could cause retrogression of light energy capture and transmission capability, leading to a massive decrease in photosynthesis capability and even cell death. Fv/Fm is a sensitive indicator of stress in oxygenic photosynthetic organisms (H.A. Baumann et al., 2009). In this study, we found that the Fv/Fm value was decreased under K^+ stressful conditions. On the other hand, K^+ deficiency can also significantly down-regulate several proteins in both PS I and II (Fig. S3 c). ATP synthases display specialized features that represent adaptations to specific environments encountered (Lu et al., 2014). Our results showed that the content of ATP synthase was reduced over 50% in the K^+ absence treatment at the end of the experiment (Fig. 3 d). In particular, ATP synthases from photosynthetic organisms carry an inserted sequence of approximately 35 amino acids in subunit γ, which allows for redox regulation to adjust the enzyme's activity to the available light intensity (Evron et al., 2000). In most bacteria, three different subunits are arranged with a stoichiometry of ab2c9-15, in which a ring of multiple c-subunits sits at the bottom of the central stalk and is held against subunit a by the peripheral stalk, which itself is composed of two copies of subunit b (Guo and Rubinstein, 2018) and is quite sensitive to K^+ stress. *M. aeruginosa* incubated without K^+ addition caused 28% and 24% downregulation of ATP synthase subunit a and ATP synthase subunit delta. Meanwhile, excessive K^+ exposure was responsible for an 18% downregulation of ATP synthase subunit b, which could restrain the production of ATP and the photosynthesis capability. Moreover, when culturing *M. aeruginosa* in the K^+ = 0.92 mM medium, the photosystem I reaction center subunit XII was also down-regulated by 22%. Table S3 shows altered protein expressions related to photosystems were associated with PS II, indicating the greater sensitivity of PS II than PS I, an observation supported by the first investigation of the role of K^+ in *M. aeruginosa* growth (Shukla and Rai, 2006). Therefore, we can infer that deficient or excessive available K^+ can restrain photosystems of *M. aeruginosa*.

4.4. K^+ stress regulates the MC-producing ability of M. aeruginosa

It has been found that MC contributes to photosynthesis, environmental adaptation, and nutrient metabolism and storage for *M. aeruginosa* (Omidi et al., 2018). Meanwhile, MC-producing capability can be regulated by a wide range of factors such as available nutrient concentrations, light and temperature (Otten et al., 2012). Moreover, it was found that the oxidative damage of *M. aeruginosa* may impel the cells to synthesis more intracellular MC and facilitated the release of MC to the surrounding environment through membrane leakage (Merel et al., 2013). In the present study, similar phenomena appeared at day 6, the MDA level of the 0.23 mM treatment showed a distinct increase, meanwhile the EMC and IMC were significantly up-regulated, among which the EMC at day 12 was even 1.11 times of the control. However, EMC and IMC level failed to increase with the oxidative stress in the K^+ absent treatment, we assume that this is mainly because of the severe intracellular energy deficiency, which limited the MC-producing

ability of *M. aeruginosa*, which can be supported by the result of ATP synthase assay. At the end of the experiment (day 30), the EMC level showed a dramatic increase with elevated K^+ concentrations (Fig. 3 a), and the expression of MC-producing genes displayed almost the same trend as the MC profile. It was worth noting that despite the transcriptional levels of *mcy*A, B and H in the K^+ = 0.92 mM treatment group were significantly higher than those in the K^+ = 0.46 mM group (p < 0.05) (Fig. 3 e), and the final algal density accounted for approximately 80% of that in the control (Fig. 1 a), which may consequently have led to an insignificant difference in the yield of the EMC level. Additionally, *mcy*H is considered to be the ABC transporter gene and is responsible for MC release (Zhou et al., 2017). In the current study, the transcriptional levels of *mcy*H in *M. aeruginosa* incubated without K^+ amendment was approximately 50% less than the control, which would significantly reduce the MC release and further decrease the EMC level. Besides, the decrease of Fd and ATP synthetase level might also contributed to the inhibition of energy supply and inhibit the biosynthesis and transportation process of MC. Nevertheless, little literature is available on the specific mechanisms by which K^+ causes variation of the MC-producing capability of *M. aeruginosa*.

It has been proven that iron limitation has a negative effect on photosynthetic capacity and *mcy* gene expressions (Wang et al., 2018). Under the favorable K^+ scenario (K^+ = 0.46 mM), the iron (III) transport system substrate-binding protein (AfuA), an important iron transport protein that directly determines the cellular uptake of iron (III) (Alvarez Hayes et al., 2013), can transport the aqueous Fe^{3+} into the cyanobacterial cells (Fig. 5 a1). Moreover, Fd, a photosynthetic protein that serves as an electron donor in the photosynthetic electron transport chain (Buckel and Thauer, 2013) (Fig. 5 a2), is also essential for ATP production. Additionally, it was previously demonstrated that MC biosynthesis requires energy that is mostly contributed by ATP produced by photosynthesis activities (Fig. 5 a3) (Wilson et al., 2006). As a result, the alternation of photosynthetic efficiency may influence the *mcy* genes expression and, consequently MC biosynthesis, which can be regulated by the *mcy* gene cluster. The *mcy*A and *mcy*B encode the extension of the dipeptidyl intermediate to the heptapeptidyl step and subsequent peptide cyclization in MC chemical construction, in which iron availability can benefit the transcription of *mcy*A (Wang et al., 2018) (Fig. 5 a4). The gene *mcy*D encodes the formation of the pentaketide-derived L-amino acid Adda and its linkage to D-glutamate (Tillett et al., 2000), and the expression of *mcy*H, a putative ABC transporter, was proposed to function as an exporter of the intracellular MC (Qian et al., 2012). Briefly, the expression of *mcy*A, B and D is imperative for the biosynthesis of MC (Fig. 5 a5), while *mcy*H influences the MC releasing capability (Fig. 5 a6).

In our study, it was proven that K^+ deficiency decreased both MC release (Fig. 2 a) and photosynthetic efficiency (Fig. S3 c), and a hypothesis regarding the relationship between available K^+ concentration and MC biosynthesis in *M. aeruginosa* was proposed (Fig. 5 b). With the absence of K^+, several iron-related proteins, including AfuA, Ferredoxin and Ferredoxin-1, were remarkably down-regulated (Table S2 and 3). In particular, AfuA was down-regulated by 34%, which lead to a severe inhibition of the uptake of iron (III) ions in *M. aeruginosa* cells (Fig. 5 b1). As a result, down-regulation of Fd (Fig. 5 b2) was triggered, which broke the photosynthesis electron transport chain and induced a decrease in ATP production, as revealed by the down-regulated ATP synthases (a and delta) (Fig. 5 b3). This was in good agreement with previous literature, which found that iron limitation has a negative impact on growth rate and energy metabolism in *M. aeruginosa* due to the down-regulation of photosynthesis proteins and pigments (Wang et al., 2010). Hence, with the impairment of AfuA expression and
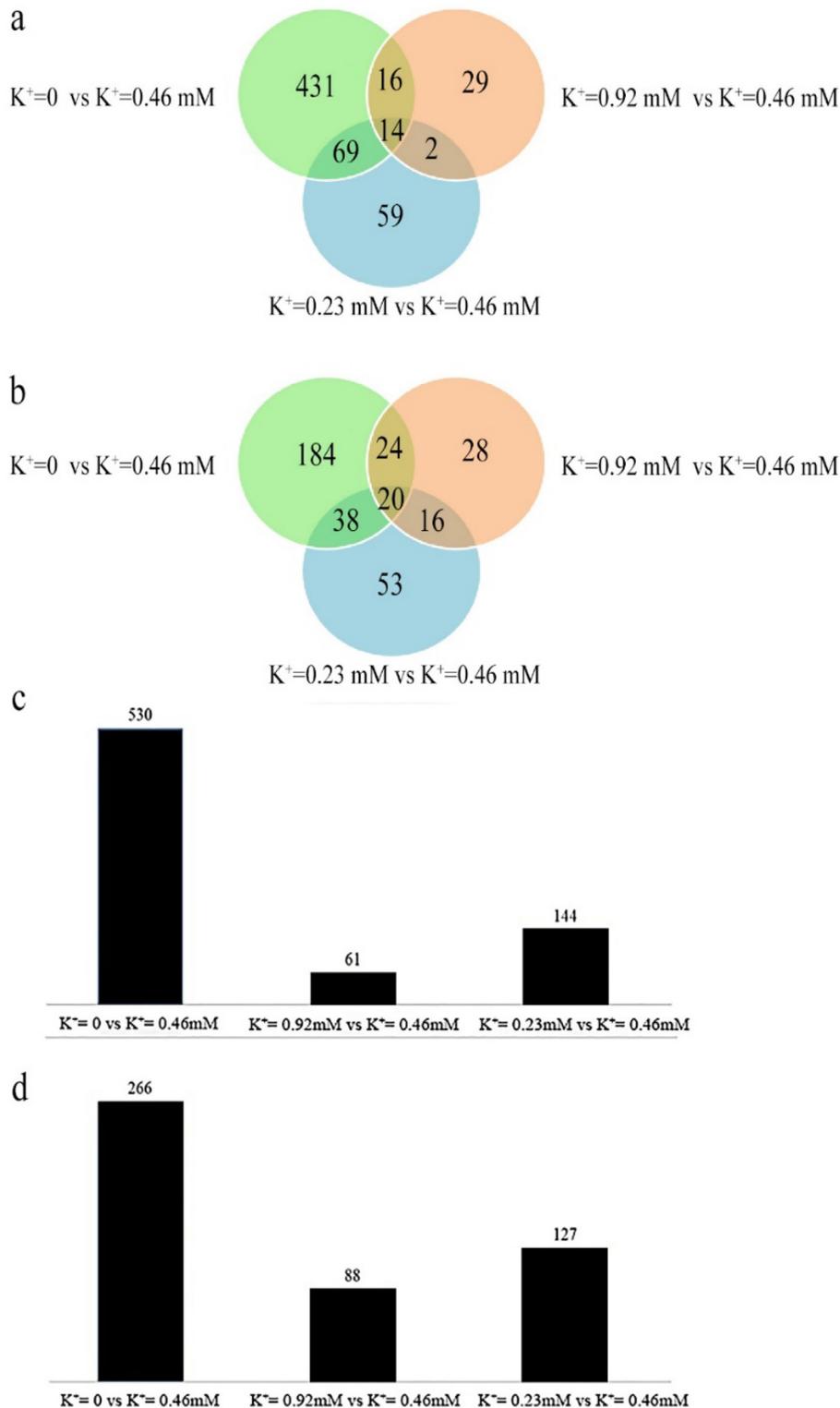
Fig. 4. Venn diagrams and histogram of regulated proteins detected under the studied K$^+$ concentrations. a, c: upregulated proteins compared with *M. aeruginosa* incubated in BG-11 medium, b, d revealed proteins that were downregulated.

photosynthesis activity, the down-regulation of *mcy* genes was observed. Depleted K$^+$ availability caused the synchronous variation of iron assimilation, which was responsible for the down-regulation of *mcy*A (Fig. 5 b4), associated with the negatively impacted the expression of *mcy*B and D (Fig. 5 b5), the biosynthesis

of MC was substantially depressed (Fig. 5 b6). Moreover, as the downregulation of *mcy*H (which functions as an exporter of the intracellular MC), the release of the intracellular MC was inhibited (Fig. 5 b7), which explained the minimum concentration of EMC in the absence of K$^+$ in BG-11 medium (Fig. 2 a). Based on the available
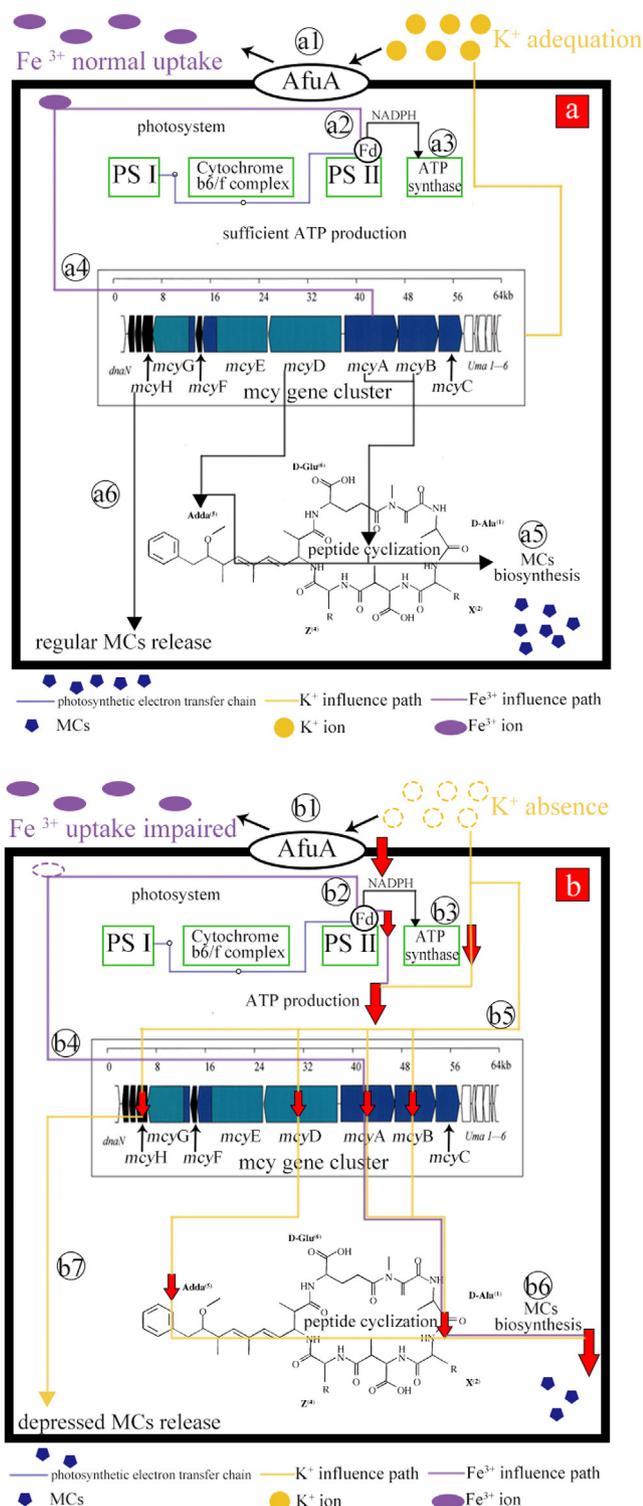
Fig. 5. Conceptual schematic of MC biosynthesis and release by *M. aeruginosa* under favorable (a) and deficient (b) K$^+$ conditions.

data, we found that both MC synthesis and MC transport were depressed in the scenario of K$^+$ absence, which jointly led to the reduced MC concentration in the solution.

4.5. Environmental implications

In our study, the growth dynamics of *M. aeruginosa* (Fig. 1), the alternation of *M. aeruginosa* cell integrity (Fig. S4) and the response of *Microcystis* physiology (Fig. S3) jointly confirmed the dual role of K$^+$ in the growth of *M. aeruginosa*; demonstrating that *M. aeruginosa* incubated in the absence of K$^+$ or in K$^+$-deficient medium (in comparison to K$^+$ = 0.46 mM medium) led to a substantial decreases of both *M. aeruginosa* density and MC production. Thus, K$^+$ appears to hold excellent potential for the control of *Microcystis* biomass and MC content in fresh water. The range of K$^+$ concentrations in natural fresh water is wide (0.1–1000 μM) (Jaworski et al., 2003), which is close to the studied K$^+$ concentrations here (0–920 μM). Previous study indicated that K$^+$ can be used as an indicator for potential sources of contamination, attributed mainly to anthropogenic activities including agricultural land use and discharge of treated wastewater, and K$^+$ losses from agroecosystems may lead into higher K$^+$ concentration in the surface waters (Skowron et al., 2018). Based on the observation that K$^+$ deficiency exhibited a negative impact on *M. aeruginosa* growth, and the precedent of the success of Phoslock™, which was developed to remove phosphorus compounds in eutrophic waters and to reduce algae growth (Kasprzyk et al., 2018). Therefore, controlling cyanobacterial HABs through the regulation of K$^+$ concentration in natural waters would likely be effective if "Potassium-lock" could be successfully developed. However, this requires further systematic investigation in both laboratory and field conditions.

5. Conclusion

This study examined the impact of K$^+$ concentration on the growth, oxidative stress and toxin-producing ability of *M. aeruginosa*. In comparison to *M. aeruginosa* incubated with favorable K$^+$ concentrations (control, K$^+$ = 0.46 mM), varied K$^+$ concentration stress posed negative impact on growth and oxidative stress of *M. aeruginosa* in different degrees, among which K$^+$ depletion exhibited most severe inhibition to *M. aeruginosa* growth. This was achieved through the downregulation of photosynthesis and ABC-transporter proteins such as Ferredoxin, AfuA, and ATP synthase subunits. Moreover, in the K$^+$-absent treatment, serious oxidative damage was noted and the biosynthesis of MC in *M. aeruginosa* cells was remarkably impaired. In addition, the transcription of *mcy*H, which functions as an exporter of the intracellular MC, was reduced by 85.89% in comparison to the control. However, with increasing K$^+$ concentration (double that of the favorable dose), photosynthesis efficiency, the expression of ABC-transporter proteins, and the transcription of *mcy* genes of *M. aeruginosa* seemed to display slight differences relative to the control. This study showed for the first time the role of the available K$^+$ concentration in regulating the growth and oxidative stress of *M. aeruginosa* and explore the possible pathway of how the K$^+$-absent condition inhibit the MC biosynthesis ability of *M. aeruginosa*.

Author statement

Yixin He: Conceptualization, Methodology, Data curation, Writing- Reviewing and Editing. Jianrong Ma: Data curation. Vanderwall Joseph: Writing- Reviewing and Editing. Yanyan Wei: Conceptualization. Mengzi Liu: Data curation. Zhaoxue Zhang: Formal analysis. Guo Li: Methodology. Qiang He: Writing - original draft. Hong Li: Data curation, Writing- Reviewing and Editing, Funding acquisition.

Declaration of competing interest

Acknowledgments

Appendix A. Supplementary data

Supplementary data to this article can be found online at https://doi.org/10.1016/j.envpol.2020.115576.

References

Alvarez Hayes, J., Erben, E., Lamberti, Y., Principi, G., Maschi, F., Ayala, M., Rodriguez, M.E., 2013. Bordetella pertussis iron regulated proteins as potential vaccine components. Vaccine 31, 3543–3548.

Bai, X., Sun, J., Zhou, Y., Gu, L., Zhao, H., Wang, J., 2017. Variations of different dissolved and particulate phosphorus classes during an algae bloom in a eutrophic lake by 31 P NMR spectroscopy. Chemosphere 169, 577–585.

Barros, M.U.G., Wilson, A.E., Leitão, J.I.R., Pereira, S.P., Buley, R.P., Fernandez-Figueroa, E.G., Capelo-Neto, J., 2019. Environmental factors associated with toxic cyanobacterial blooms across 20 drinking water reservoirs in a semi-arid region of Brazil. Harmful Algae 86, 128–137.

Baumann, H.A., Morrison, L., Stengel, D.B., 2009. Metal accumulation and toxicity measured by PAM—chlorophyll fluorescence in seven species of marine macroalgae. Ecotoxicol. Environ. Saf. 72, 1063–1075.

Beklioglu, M., Moss, B., 2010. The impact of pH on interactions among phytoplankton algae, zooplankton and perch (Perca fluviatilis) in a shallow, fertile lake. Freshw. Biol. 33, 497–509.

Brdjanovic, D., Hooijmans, C.M., van Loosdrecht, M.C.M., Alaerts, G.J., Heijnen, J.J., 1996. The dynamic effects of potassium limitation on biological phosphorus removal. Water Res. 30, 2323–2328.

Buckel, W., Thauer, R.K., 2013. Energy conservation via electron bifurcating ferredoxin reduction and proton/Na+ translocating ferredoxin oxidation. BBA-Bioenergetics 1827, 94–113.

Chen, C., Yang, Z., Kong, F., Zhang, M., Yu, Y., Shi, X., 2016. Growth, physiochemical and antioxidant responses of overwintering benthic cyanobacteria to hydrogen peroxide. Environ. Pollut. 219, 649–655.

Demirel, S., Ustun, B., Aslim, B., Suludere, Z., 2009. Toxicity and uptake of iron ions by synechocystis sp. E35 isolated from kucukcekmece lagoon. Istanbul. J. Hazard. Mater. 171, 710–716.

Do, T.H.T., Martinoia, E., Lee, Y., 2018. Functions of ABC transporters in plant growth and development. Curr. Opin. Plant Biol. 41, 32–38.

Du, B., Liu, G., Ke, M., Zhang, Z., Zheng, M., Lu, T., Sun, L., Qian, H., 2019. Proteomic analysis of the hepatotoxicity of Microcystis aeruginosa in adult zebrafish (Danio rerio) and its potential mechanisms. Environ. Pollut. 254, 113019.

Evron, Y., Johnson, E.A., McCarty, R.E., 2000. Regulation of proton flow and ATP synthesis in chloroplasts. J. Bioenerg. Biomembr. 32, 501–506.

Fontanillo, M., Köhn, M., 2018. Microcystins: synthesis and structure–activity relationship studies toward PP1 and PP2A. Bioorg. Med. Chem. 26, 1118–1126.

Fu, Q.L., Fujii, M., Natsuike, M., Waite, T.D., 2019. Iron uptake by bloom-forming freshwater cyanobacterium Microcystis aeruginosa in natural and effluent waters. Environ. Pollut. 247, 392–400.

Guo, H., Rubinstein, J.L., 2018. Cryo-EM of ATP synthases. Curr. Opin. Struct. Biol. 52, 71–79.

Hassan, H.M., Scandalios, J.M., 1990. Superoxide dismutases in aerobic organisms. In: Alscher, R.G., Cumming, J.R. (Eds.), Stress Responses in Plants: Adaptation and Acclimatation Mechanisms. Wiley-Liss, New York, pp. 175–199.

He, Q., Kang, L., Sun, X., Jia, R., Zhang, Y., Ma, J., Li, H., Ai, H., 2018. Spatiotemporal distribution and potential risk assessment of microcystins in the Yulin River, a tributary of the Three Gorges Reservoir, China. J. Hazard. Mater. 347, 184–195.

Hernandez, M., Fernandez-Garcia, N., Garcia-Garma, J., Rubio-Asensio, J.S., Rubio, F., Olmos, E., 2012. Potassium starvation induces oxidative stress in Solanum lycopersicum L. roots. J. Plant Physiol. 169, 1366–1374.

Hu, S., Yu, Y., Wu, X., Xia, X., Xiao, X., Wu, H., 2017. Comparative proteomic analysis of Cronobacter sakazakii by iTRAQ provides insights into response to desiccation. Food Res. Int. 100, 631–639.

Inda, L.A., Luisa Peleato, M., 2003. Development of an ELISA approach for the determination of flavodoxin and ferredoxin as markers of iron deficiency in phytoplankton. Phytochemistry 63, 303–308.

Jaworski, G.H.M., Talling, J.F., Heaney, S.I., 2003. Potassium dependence and phytoplankton ecology: an experimental study. Freshw. Biol. 48, 833–840.

Kasprzyk, M., Obarska-Pempkowiak, H., Masi, F., Gajewska, M., 2018. Possibilities of Phoslock® application to remove phosphorus compounds from wastewater treated in hybrid wetlands. Ecol. Eng. 122, 84–90.

Knutson, C.M., McLaughlin, E.M., Barney, B.M., 2018. Effect of temperature control on green algae grown under continuous culture. Algal Res 35, 301–308.

Kobayashi, T., Nozoye, T., Nishizawa, N.K., 2019. Iron transport and its regulation in plants. Free Radical Bio. Med. 133, 11–20.

Livak, K.J., Schmittgen, T.D., 2001. Analysis of relative gene expression data using real-time quantitative PCR and the 2(-Delta Delta C(T)) Method. Methods 25, 402–408.

Lu, P., Lill, H., Bald, D., 2014. ATP synthase in mycobacteria: special features and implications for a function as drug target. BBA Bioenergetics 1837, 1208–1218.

Mao, Y., Ai, H., Chen, Y., Zhang, Z., Zeng, P., Kang, L., Li, W., Gu, W., He, Q., Li, H., 2018. Phytoplankton response to polystyrene microplastics: perspective from an entire growth period. Chemosphere 208, 59–68.

Melegari, S.P., Perreault, F., Costa, R.H., Popovic, R., Matias, W.G., 2013. Evaluation of toxicity and oxidative stress induced by copper oxide nanoparticles in the green alga Chlamydomonas reinhardtii. Aquat. Toxicol. 142, 431–440.

Merel, S., Walker, D., Chicana, R., Snyder, S., Baurès, E., Thomas, O., 2013. State of knowledge and concerns on cyanobacterial blooms and cyanotoxins. Environ. Int. 59, 303–327.

Omidi, A., Esterhuizen-Londt, M., Pflugmacher, S., 2018. Still challenging: the ecological function of the cyanobacterial toxin microcystin — what we know so far. Toxin Rev. 37, 87–105.

Otten, T.G., Xu, H., Qin, B., Zhu, G., Paerl, H.W., 2012. Spatiotemporal patterns and ecophysiology of toxigenic Microcystis blooms in lake taihu, China: implications for water quality management. Environ. Sci. Technol. 46, 3480–3488.

Pearson, L.A., Michael, H., Thomas, B.R., Elke, D., Neilan, B.A., 2004. Inactivation of an ABC transporter gene, mcyH, results in loss of microcystin production in the cyanobacterium Microcystis aeruginosa PCC 7806. Appl. Environ. Microbiol. 70, 6370–6378.

Plato, P., Denovan, J.T., 1974. The influence of potassium on the removal of 137 Cs by live Chlorella from low level radioactive wastes. Radiat. Bot. 14, 37–41.

Qian, H., Pan, X., Chen, J., Zhou, D., Chen, Z., Zhang, L., Fu, Z., 2012. Analyses of gene expression and physiological changes in Microcystis aeruginosa reveal the phytotoxicities of three environmental pollutants. Ecotoxicology 21, 847–859.

Qiu, H., Geng, J., Ren, H., Xia, X., Wang, X., Yu, Y., 2013. Physiological and biochemical responses of Microcystis aeruginosa to glyphosate and its roundup formulation. J. Hazard. Mater. 248–249, 172–176.

Rochaix, J.D., 2007. Role of thylakoid protein kinases in photosynthetic acclimation. FEBS Lett. 581, 2768–2775.

Sandgreen, C.D., 1988. The Ecology of Chrysophyte Flagellates : Their Growth and Perennation Strategies as Freshwater Phytoplankton. Cambridge University Press, pp. 9–104.

Seip, K.L., 1994. Phosphorus and nitrogen limitation of algal biomass across trophic gradients. Aquat. Sci. 56, 16–28.

Sheng, H., Niu, X., Song, Q., Li, Y., Zhang, R., Zou, D., Lai, S., Yang, Z., Tang, Z., Zhou, S., 2019. Physiological and biochemical responses of Microcystis aeruginosa to phosphine. Environ. Pollut. 247, 165–171.

Shukla, B., Rai, L.C., 2006. Potassium-induced inhibition of photosynthesis and associated electron transport chain of Microcystis: implication for controlling cyanobacterial blooms. Harmful Algae 5, 184–191.

Skowron, P., Skowrońska, M., Bronowicka-Mielniczuk, U., Filipek, T., Igras, J., Kowalczyk-Juśko, A., Krzepiłko, A., 2018. Anthropogenic sources of potassium in surface water: the case study of the Bystrzyca river catchment, Poland. Agric. Ecosyst. Environ. 265, 454–460.

Smith, G.J., Daniels, V., 2018. Algal blooms of the 18th and 19th centuries. Toxicon 142, 42–44.

Talling, J.F., 2010. Potassium — a non-limiting nutrient in fresh waters? Freshwater Rev 3, 97–104.

Tillett, D., Dittmann, E., Erhard, M., von Döhren, H., Börner, T., Neilan, B.A., 2000. Structural organization of microcystin biosynthesis in Microcystis aeruginosa PCC7806: an integrated peptide–polyketide synthetase system. Chem. Biol. 7, 753–764.

Vanhoudt, N., Cuypers, A., Horemans, N., Remans, T., Opdenakker, K., Smeets, K., Bello, D.M., Havaux, M., Wannijn, J., Van Hees, M., Vangronsveld, J., Vandenhove, H., 2011. Unraveling uranium induced oxidative stress related responses in Arabidopsis thaliana seedlings. Part II: responses in the leaves and general conclusions. J. Environ. Radioact. 102 (6), 638–645.

Wang, C., Kong, H.N., Wang, X.Z., Wu, H.D., Lin, Y., He, S.B., 2010. Effects of iron on growth and intracellular chemical contents of Microcystis aeruginosa. Biomed.

Environ. Sci. 23, 48—52.

Wang, Y., Min, W., Jing, Y., Zhang, J., Zhang, R., Lu, Z., Chen, G., Wang, Y., Min, W., Jing, Y., 2014. Differences in growth, pigment composition and photosynthetic rates of two phenotypes Microcystis aeruginosa strains under high and low iron conditions. Biochem. Systemat. Ecol. 55, 112—117.

Wang, X., Wang, P., Wang, C., Hu, B., Ren, L., Yang, Y., 2018. Microcystin biosynthesis in Microcystis aeruginosa: indirect regulation by iron variation. Ecotox. Environ. Safe. 148, 942—952.

Wilson, K.E., Ivanov, A.G., Oquist, G., Grodzinski, B., Sarhan, F., Huner, N.P.A., 2006. Energy balance, organellar redox status, and acclimation to environmental stress. Can. J. Bot. 84, 1355—1370.

Winter, U., Meyer, M.I.B., Kirst, G.O., 1987. Seasonal changes of ionic concentrations in the vacuolar sap of Chara vulgaris L. growing in a brackish water lake. Oecologia 74, 122—127.

Yan, X., Xu, X., Wang, M., Wang, G., Wu, S., Li, Z., Sun, H., Shi, A., Yang, Y., 2017. Climate warming and cyanobacteria blooms: looks at their relationships from a new perspective. Water Res. 125, 449—457.

Yang, L.T., Qi, Y.P., Lu, Y.B., Guo, P., Sang, W., Feng, H., Zhang, H.X., Chen, L.S., 2013. iTRAQ protein profile analysis of Citrus sinensis roots in response to long-term boron-deficiency. J. Proteomics 93, 179—206.

Zhang, H., Yang, L., Yu, Z., Huang, Q., 2014. Inactivation of Microcystis aeruginosa by DC glow discharge plasma: impacts on cell integrity, pigment contents and microcystins degradation. J. Hazard Mater. 268, 33—42.

Zheng, L., Zhang, X., Bai, Y., Fan, J., 2018. Using algae cells to drive cofactor regeneration and asymmetric reduction for the synthesis of chiral chemicals. Algal Res 35, 432—438.

Zhou, C., Huang, J.C., Liu, F., He, S., Zhou, W., 2017. Effects of selenite on Microcystis aeruginosa: growth, microcystin production and its relationship to toxicity under hypersalinity and copper sulfate stresses. Environ. Pollut. 223, 535—544.